AD-A284 951
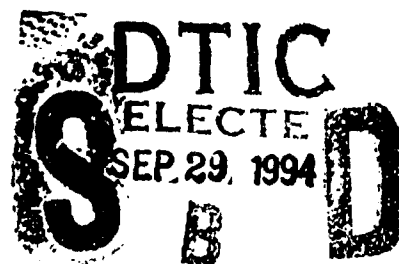
Optimum Truncation of a Gaussian Beam in the Presence of Random Jitter

15 September 1994

Prepared by

H. T. YURA
Electronics Technology Center
Technology Operations

DTIC
ELECTE
SEP. 29, 1994
S
B
D

Prepared for

SPACE AND MISSILE SYSTEMS CENTER
AIR FORCE MATERIEL COMMAND
2430 E. El Segundo Boulevard
Los Angeles Air Force Base, CA 90245

Engineering and Technology Group

94-31013

THE AEROSPACE
CORPORATION
El Segundo, California

94 9 28 0 45

REPORT DOCUMENTATION PAGE

Form Approved
OMB No. 0704-0188

1. AGENCY USE ONLY (*Leave blank*)	2. REPORT DATE 15 September 1994	3. REPORT TYPE AND DATES COVERED

4. TITLE AND SUBTITLE
Optimum Truncation of a Gaussian Beam in the Presence of Random Jitter

5. FUNDING NUMBERS
F04701-93-C-0094

6. AUTHOR(S)
H. T. Yura

7. PERFORMING ORGANIZATION NAME(S) AND ADDRESS(ES)
The Aerospace Corporation
Technology Operations
El Segundo, CA 90245-4691

8. PERFORMING ORGANIZATION REPORT NUMBER
TR-94(4925)-4

9. SPONSORING/MONITORING AGENCY NAME(S) AND ADDRESS(ES)
Space and Missile Systems Center
Air Force Materiel Command
2430 E. El Segundo Boulevard
Los Angeles Air Force Base, CA 90245

10. SPONSORING/MONITORING AGENCY REPORT NUMBER
SMC-TR-94-35

11. SUPPLEMENTARY NOTES

12a. DISTRIBUTION/AVAILABILITY STATEMENT
Approved for public release; distribution unlimited

12b. DISTRIBUTION CODE

13. ABSTRACT (*Maximum 200 words*)

We consider the far-field (or focal-plane) irradiance distribution of a Gaussian beam truncated by a circular aperture in the presence of random angular jitter. First, in the absence of jitter, we derive an accurate analytical approximation for the irradiance distribution within the main lobe of the beam for the case where the beam diameter is less than the aperture diameter. We then obtain the corresponding mean irradiance distribution in the presence of circularly symmetric, normally distributed jitter. By maximizing the on-axis intensity, we obtain the optimum ratio of the beam diameter to the aperture diameter in the presence of jitter and present results for the corresponding maximum on-axis intensity and encircled power as a function of the jitter statistics.

DTIC QUALITY INSPECTED 3

14. SUBJECT TERMS
Gaussian beams, Jitter

15. NUMBER OF PAGES
17

16. PRICE CODE

17. SECURITY CLASSIFICATION OF REPORT UNCLASSIFIED	18. SECURITY CLASSIFICATION OF THIS PAGE UNCLASSIFIED	19. SECURITY CLASSIFICATION OF ABSTRACT UNCLASSIFIED	20. LIMITATION OF ABSTRACT

Preface

I wish to thank Dr. S. C. Moss of The Aerospace Corporation for his helpful comments and critical reading of the manuscript.

i

Contents

Figures

1. Introduction

In many optical systems employing lasers, it is important to obtain the maximum far-field (or focal-plane) irradiance, for a given output laser power, on or near the optic axis. Examples of such systems include optical radars, where one wants to obtain the highest possible signal return, and optical communications systems, where one wishes to operate under conditions of the highest possible signal-to-noise ratio. In these systems and others, one is often concerned with the far-field radiation pattern that is well within the central lobe of the transmitted beam, the corresponding details of the much weaker side lobes being of less relative importance. Since all systems, in practice, operate in the presence of some (unintentional) random angular jitter, it is of concern to know what the optimum truncation of the laser output beam should be in order to obtain the highest possible average on-axis, far-field irradiance. Here, random angular jitter (e.g., due to random vibrations of the optical platform mount and propagation through the atmosphere where clear air turbulence-induced wave-front tilt produces effects formally equivalent to random platform jitter[1]) refers to the uncertainty of the instantaneous direction of the optical axis with respect to a nominal z-axis that is parallel to the direction of the desired line of sight.

Specifically, here we model random angular jitter by the commonly used assumption that it is normally distributed about both the x- and y-axes with zero mean and equal variances. As we show below, the far-field beam pattern of a truncated Gaussian is, over the parameter range of interest here, very nearly of Gaussian shape. This, together with the assumption of normally distributed jitter, allows one to obtain an analytical expression for the corresponding average beam irradiance distribution in the presence of jitter. Maximizing the on-axis mean irradiance as a function of the ratio of the beam diameter in the aperture to the truncation diameter yields the optimum value of the beam diameter for a given aperture diameter.

In Section 2, we present a general expression for the far-field irradiance distribution in the paraxial approximation of a circular aperture illuminated by a Gaussian beam in the absence of jitter. We then briefly review the well-known optimum truncation of the beam through a fixed circular aperture. Next, we derive an accurate analytical approximation within the central lobe of the exact irradiance distribution over a parameter range of interest. Based on this approximation, in Section 3, we derive a corresponding analytical approximation for the mean irradiance distribution in the presence of random jitter. We then maximize the mean on-axis irradiance as a function of the ratio of the beam diameter in the aperture to the aperture diameter to obtain the optimum value of the beam diameter that yields the corresponding maximum mean on-axis irradiance in the presence of jitter. Previously, optical systems modelers have often had to resort to complex and time consuming numerical procedures (e.g., Monte Carlo techniques) to account for random jitter. The accurate elementary approximations obtained here allow analytical results to be obtained for the optimum mean irradiance distribution in the presence of random jitter, which, in many cases, aids in facilitating parametric estimation and optimization of overall system performance.

2. Far-Field Irradiance Distribution in the Absence of Jitter

In this report, we consider an unobscured circular aperture of diameter D that truncates a (TEM$_{00}$) Gaussian-shaped laser beam of $1/e^2$ intensity, radius ω_0, and power P. In the absence of jitter, the irradiance distribution of wavelength λ at propagation distance R in the far field (i.e., for propagation distances satisfying $R \gg \pi\omega_0^2/\lambda$) at angular coordinate θ, can be expressed as[2]

$$I(\theta) = I(0)G(\theta), \tag{2.1}$$

where I(0), the on-axis irradiance, is given by

$$I(0) = I_U F_{trunc}, \tag{2.2}$$

$$I_U = \frac{PA}{(\lambda R)^2}, \tag{2.3}$$

$$F_{trunc} = \frac{2[1 - \exp\{-\mu^2\}]^2}{\mu^2}, \tag{2.4}$$

A is the area of the aperture (= $\pi D^2/4$), and G(θ), the normalized beam pattern, is given by

$$G(\theta) = \left[\frac{2\int_0^\mu dx\, x \exp\left(-x^2\right) J_0(ux/\mu)}{1 - \exp\left(-\mu^2\right)} \right]^2, \tag{2.5}$$

where J$_0$ is the Bessel function of the first kind of order zero,

$$u = \frac{\theta}{(\lambda/\pi D)}, \tag{2.6}$$

$$\mu = \frac{D}{d}, \tag{2.7}$$

and d = 2ω_0 is the beam diameter in the plane of the aperture. In Eq. (2.2), the quantity I$_U$ is the on-axis irradiance obtained for uniform illumination of the circular aperture (which is the abso-

3

lute maximum on-axis irradiance obtained under any physical circumstances), and the quantity F_{trunc} gives the effects of truncation of the Gaussian beam by the aperture. For an aperture of fixed diameter D, it is well known[2] that the maximum on-axis, far-field irradiance is obtained for $d \approx 0.89D$. For this value of d, $F_{trunc} \approx 0.81$. Thus, in the absence of jitter, the maximum far-field intensity is about 81% of what would be obtained if the same total power is uniformly distributed over the circular aperture; this condition occurs for $d/D \approx 0.89$.

As is shown in Section 3, the optimum value of d/D in the presence of jitter is obtained for $(d/D)_{opt} < 0.89$. As such, we first derive an accurate expression for the beam pattern within the central lobe for d/D < 1.

Consider a beam of Gaussian shape of the form

$$I_A(\theta) = I(0)G_A(\theta), \tag{2.8}$$

where I(0), the exact on-axis, far-field irradiance, is given by Eq. (2.2), and

$$G_A(\theta) = \exp\left[-\frac{1}{2}(\theta^2/\theta_B^2)\right], \tag{2.9}$$

where

$$\theta_B^2 = \left(\frac{\lambda}{\pi d}\right)^2 + \left(\frac{\lambda b}{\pi D}\right)^2, \tag{2.10}$$

and the parameter b is determined from the requirement that the integrated far-field irradiance of G_A equals the exact value of the transmitted power, P_T, of the truncated beam. We have

$$P_T = [1 - \exp(-2\mu^2)]P, \tag{2.11}$$

where $\mu = D/d$, and P is the incident power. Thus, b is obtained as

$$b = \frac{\sqrt{2}\mu}{\sqrt{\exp(\mu^2) - 1}}. \tag{2.12}$$

For d << D (i.e., μ >> 1), $b \approx 0$ and $\theta_B \approx \lambda/\pi d$, as expected physically. That is, for d << D, the expression for the approximate beam width reduces to that of an infinite Gaussian beam. On the other hand, for d >> D, $b \approx \sqrt{2}$. That is, in this limit the Gaussian width equals $\sqrt{2}\lambda/\pi D$. Clearly,

for d > D, it is expected physically that the truncated beam in the far field behaves more like an Airy pattern than a Gaussian. However, here we are only interested in beams where d/D < 1. For this case, we have compared, in Figures 1–4, the exact [based on numerical integration of Eq. (2.5)] and the approximate far-field pattern given by Eq. (2.9). Examination of these figures reveals that, within the first central lobe of the far-field pattern, $I_A(\theta)$ [given by Eq. (2.8)] is a very good approximation to the actual far-field irradiance pattern of a truncated Gaussian beam. The small differences indicated in the figures are well within the practical uncertainties that always exist for "real" Gaussian beams. We note that $I_A(\theta)$ gives both the correct on-axis irradiance and integrated power for the truncated beam. Additionally, for d/D < 1, the integrated far-field power in the first central lobe is > 95.5%,[3] and thus I_A is an accurate representation of the beam in this regime.

Note, the characteristic $1/e^2$ beam half-width angle, θ_B, can be written as

$$\theta_B = \frac{2\lambda}{\pi D_{eff}},$$ (2.13)

where

$$D_{eff} = d\sqrt{\tanh\left(D^2/2d^2\right)}.$$ (2.14)

Figure 1. Far-field irradiance beam pattern of a truncated Gaussian beam as function of normalized angular coordinate u [= $\theta/(\lambda/\pi D)$] for d/D = 0.9. The dashed and solid curves are based on the exact [i.e., Eq. (2.5)] and approximate [i.e., Eq. (2.9)] expressions for the beam pattern, respectively.
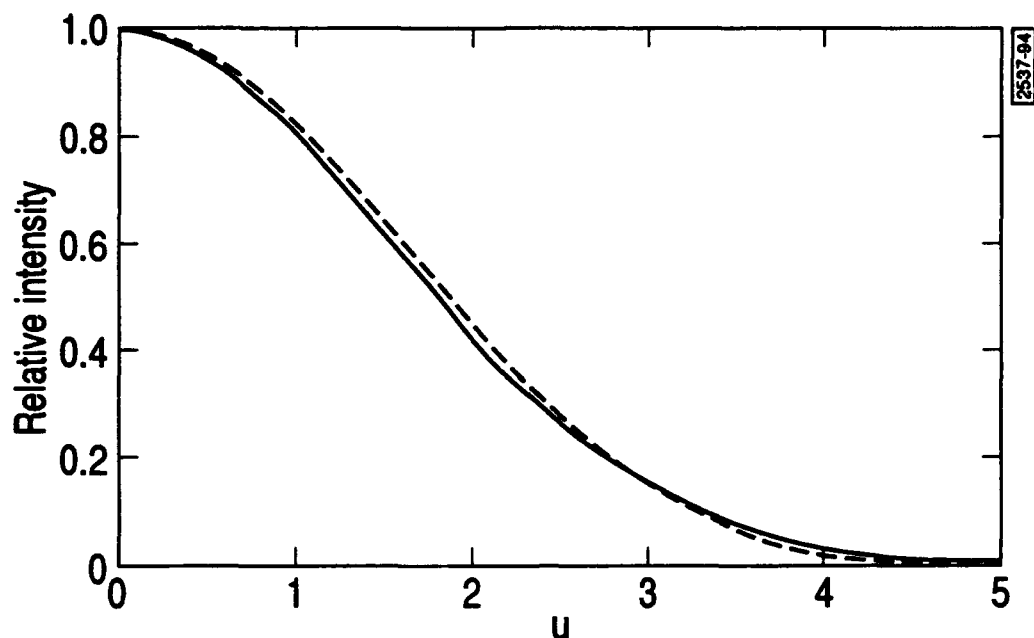
Figure 2. Far-field irradiance beam pattern of a truncated Gaussian beam as function of normalized angular coordinate u [= $\theta/(\lambda/\pi D)$] for $d/D = 0.8$. The dashed and solid curves are based on the exact [i.e., Eq. (2.5)] and approximate [i.e., Eq. (2.9)] expressions for the beam pattern, respectively.
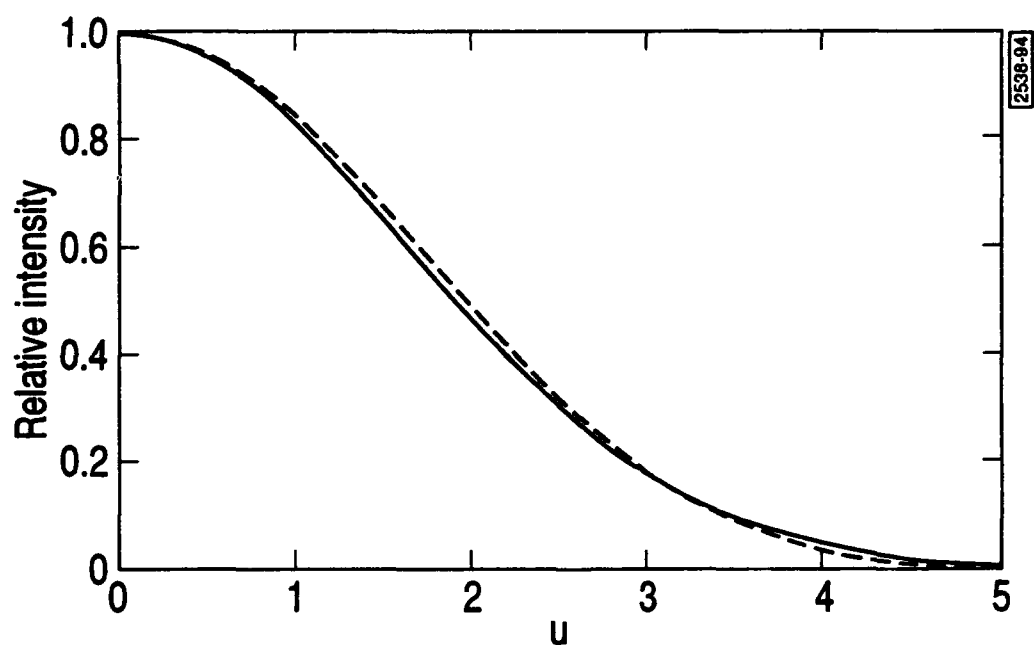
Figure 3. Far-field irradiance beam pattern of a truncated Gaussian beam as function of normalized angular coordinate u [= $\theta/(\lambda/\pi D)$] for $d/D = 0.7$. The dashed and solid curves are based on the exact [i.e., Eq. (2.5)] and approximate [i.e., Eq. (2.9)] expressions for the beam pattern, respectively.
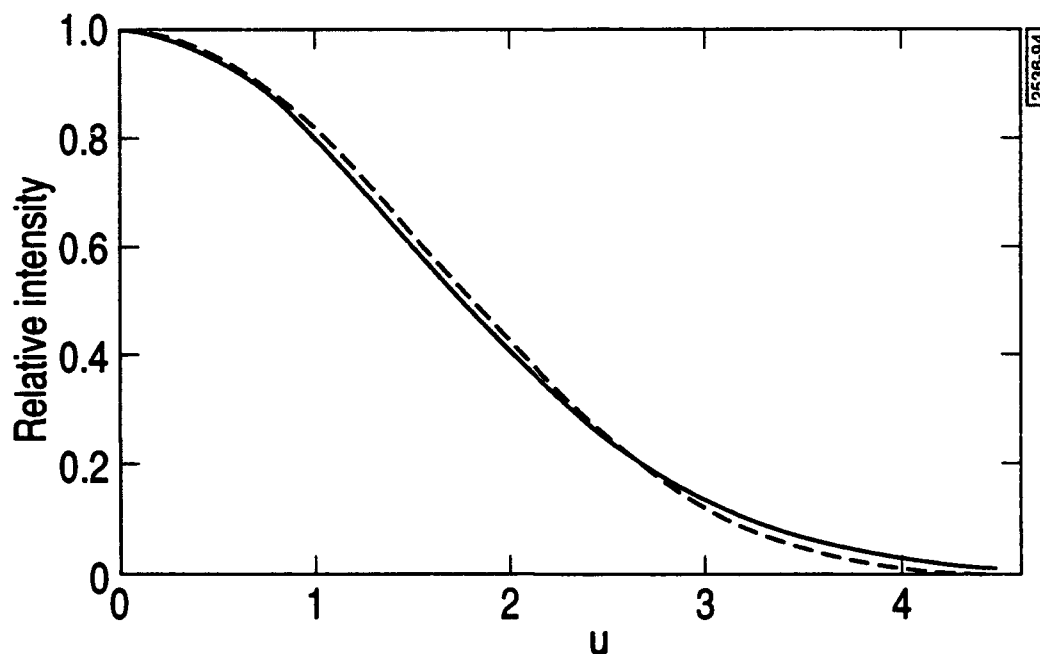
6
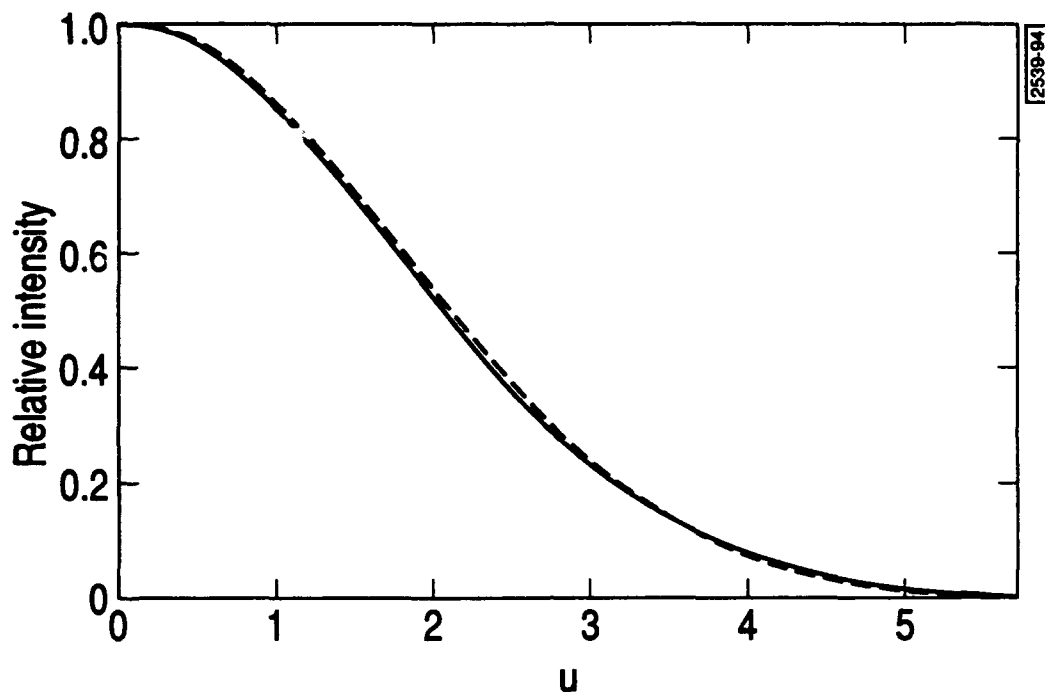
Figure 4. Far-field irradiance beam pattern of a truncated Gaussian beam as function of normalized angular coordinate u [= $\theta/(\lambda/\pi D)$] for d/D = 0.6. The dashed and solid curves are based on the exact [i.e., Eq. (2.5)] and approximate [i.e., Eq. (2.9)] expressions for the beam pattern, respectively.

The quantity D_{eff} is the $1/e^2$ beam intensity diameter in the aperture plane of an "effective" infinite Gaussian field that results in the distribution I_A. That is, we replace the original Gaussian field of $1/e^2$ diameter d and the aperture of diameter D by an infinite Gaussian field of $1/e^2$ diameter D_{eff}, which, when propagated to the far field, results in an irradiance distribution, I_A, that is a very good approximation to what would be obtained from the truncated Gaussian. We note that I_A does not correctly describe the side lobes and should not be used when the corresponding distribution is important; it is a valid approximation within the main central lobe only. In the next section, we use this infinite Gaussian field to obtain the corresponding results for the mean irradiance distribution in the presence of random angular jitter.

3. Far-Field Irradiance Distribution in the Presence of Jitter

Here, we assume circularly symmetric Gaussian angular jitter beam statistics. Let σ_j^2 denote the 1-axis, 1-σ jitter variance (for adaptive optics systems, σ_j^2 is the corresponding residual jitter variance). Then, assuming a Gaussian-shaped beam of beam width θ_B [i.e., Eq. (2.9)], it can be shown[4-6] that the average on-axis irradiance in the presence of jitter is given by

$$<I(0)> = I(0)F_{jitter} = I_U F_{trunc} F_{jitter}, \tag{3.1}$$

where

$$F_{jitter} = \frac{1}{1 + \dfrac{\sigma_j^2}{\theta_B^2}}, \tag{3.2}$$

is a reduction factor accounting for the effects of jitter on the mean on-axis far-field intensity, and angular brackets represent the ensemble average. In addition, the corresponding (approximate) mean beam profile in the presence of jitter, G_{Aj}, is given by

$$G_{Aj}(\theta) = \exp\left[-\frac{1}{2}\left(\frac{\theta^2}{\theta_B^2 + \sigma_j^2}\right)\right]. \tag{3.3}$$

For a fixed aperture diameter D, examination of Eq. (3.1) reveals that the dependence of the mean, far-field, on-axis intensity is contained in the term $F_{trunc}F_{jitter}$. Now, F_{trunc} reaches its maximum for $d \approx 0.89D$. On the other hand, F_{jitter} is a decreasing function of d. In particular, $F_{jitter}(d < 0.89D) > F_{jitter}(d > 0.89D)$. Hence, it follows that the value of d that maximizes the on-axis, far-field intensity in the presence of jitter will be obtained for $d < 0.89D$. This property is shown in Figure 5, where we have plotted $G_{Aj}(\theta)$ as function of d/D for various values of normalized jitter ρ [$= \sigma_j/(\lambda/\pi D)$].

Based on Eq. (3.1), we can readily obtain results for the optimum ratio of d/D that yields the maximum on-axis, far-field (or focal-plane) irradiance. Differentiating Eq. (3.1) with respect to "d" and setting the result equal to zero yields a transcendental equation for the optimum values of d/D:

$$2\mu_o^2 - \left(e^{\mu_o^2} - 1\right)\left[1 - \frac{2\rho^2}{\left(e^{\mu_o^2} + 1\right)^2}\right] = 0, \tag{3.4}$$
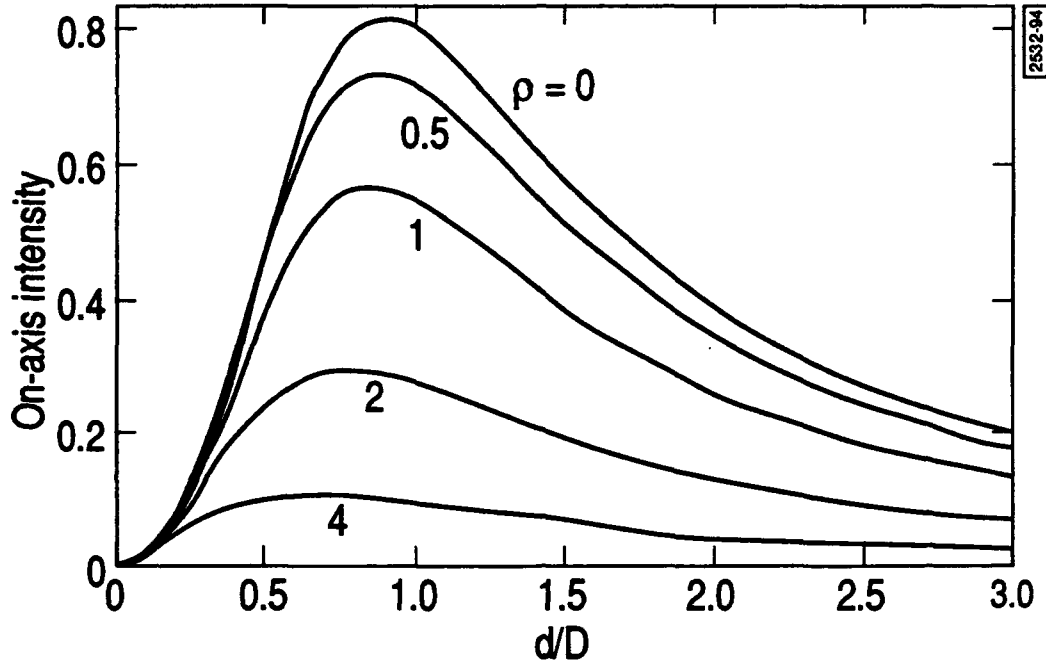
Figure 5. Far-field, on-axis irradiance as a function of d/D for various values of the normalized jitter standard deviation ρ [= $\sigma_j/(\lambda/\pi D)$, where σ_j is the 1-axis, 1-σ jitter standard deviation].

where μ_0 = (D/d)$_{opt}$, and

$$\rho = \sigma_j/(\lambda/\pi D) \tag{3.5}$$

is the normalized standard deviation of jitter.

Although Eq. (3.2) cannot be solved analytically, numerical results are readily obtained and are plotted in Figure 6 as a function of normalized jitter. Of course, for ρ = 0, the results shown in Figure 6 are identical to the results given in Chap. 18 of Ref. 1. It can be shown that for ρ >> 1, (d/D)$_{opt}$ ≈ 1/[ln(ρ)]$^{1/2}$. An accurate analytical approximation for (d/D)$_{opt}$ for 0 ≤ ρ ≤ 10, as obtained by a least-squares fit to the calculated values, is given by

$$(d/D)_{opt} = \begin{cases} 0.892 - 0.0536\rho^2 + 0.0089\rho^4 & \text{for } 0 \le \rho \le 1.3 \\ 0.468 + \dfrac{0.592}{\sqrt{\rho}} - \dfrac{0.085}{\sqrt{\ln\rho}}, & \text{for } 1.3 < 10. \end{cases} \tag{3.6}$$

The accuracy of this approximation is better than 1% over the range 0 ≤ ρ ≤ 10.

10

As a practical matter, it is expected that viable optical systems should be designed to operate in the regime of $\rho < 2$–3 or, otherwise, serious degradation of system performance by jitter will be obtained. Over this range, we obtain that $0.89 > (d/D)opt > 0.73$. For example, for $\rho = 1$ and 2, examination of Figure 6 reveals that $(d/D)_{opt} \approx 0.85$ and 0.78, respectively. Figure 7 is a plot of the optimum on-axis intensity as a function of normalized jitter. For the previous example, examination of Figure 7 reveals that for $\rho = 1$ and 2, the maximum on-axis intensity is about 57 and 30% of what would be obtained for uniform illumination of the aperture, respectively.

Another quantity of interest is the encircled transmitted power distribution. Denoting by $\Delta P(\theta_0)/P_T$ the fraction of transmitted power contained within a circle of radius θ_0, we have

$$\frac{\Delta P(\theta_0)}{P_T} = \int_0^{\theta_0} I_A(\theta) 2\pi\theta d\theta$$

$$= 1 - \exp\left(-\frac{1}{2}\frac{\theta_0^2}{\theta_B^2}\right), \tag{3.7}$$

which is plotted in Figure 8 for various values of normalized jitter, ρ. For purposes of comparison with the exact results, which are based on numerical integration of Eq. (2.5), we consider, as a worst case of interest here, the case $d/D = 0.89$ and obtain that the encircled transmitted power contained within the first central lobe is equal to 97.0% as compared with 99.2%, as obtained from the approximation given by Eq. (3.7) for $\rho = 0$. Thus, Eq. (3.7) represents a highly accurate representation for the encircled far-field (or focal plane) transmitted power distribution for all cases of interest here.
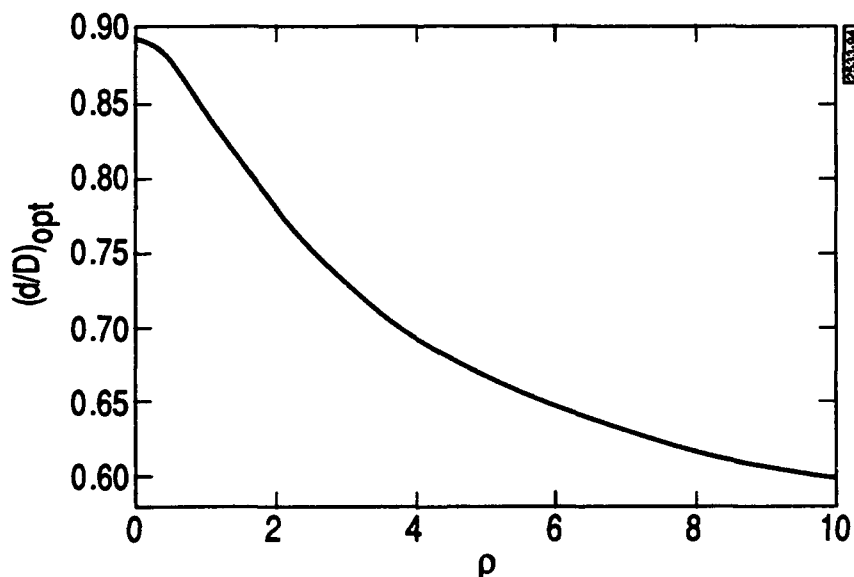
Figure 6. The optimum ratio of the beam diameter in the aperture to the truncation diameter as a function of normalized jitter.

Figure 7. The maximum mean far-field on-axis irradiance (i.e., the value for the optimum ratio of d/D) as a function of normalized jitter.

Figure 8. Encircled power distribution, $\Delta P/P_T$, as a function of normalized angular coordinate u_0 for various values of normalized jitter ρ. For each value of ρ, the beam is truncated at its optimum value.

4. Conclusions

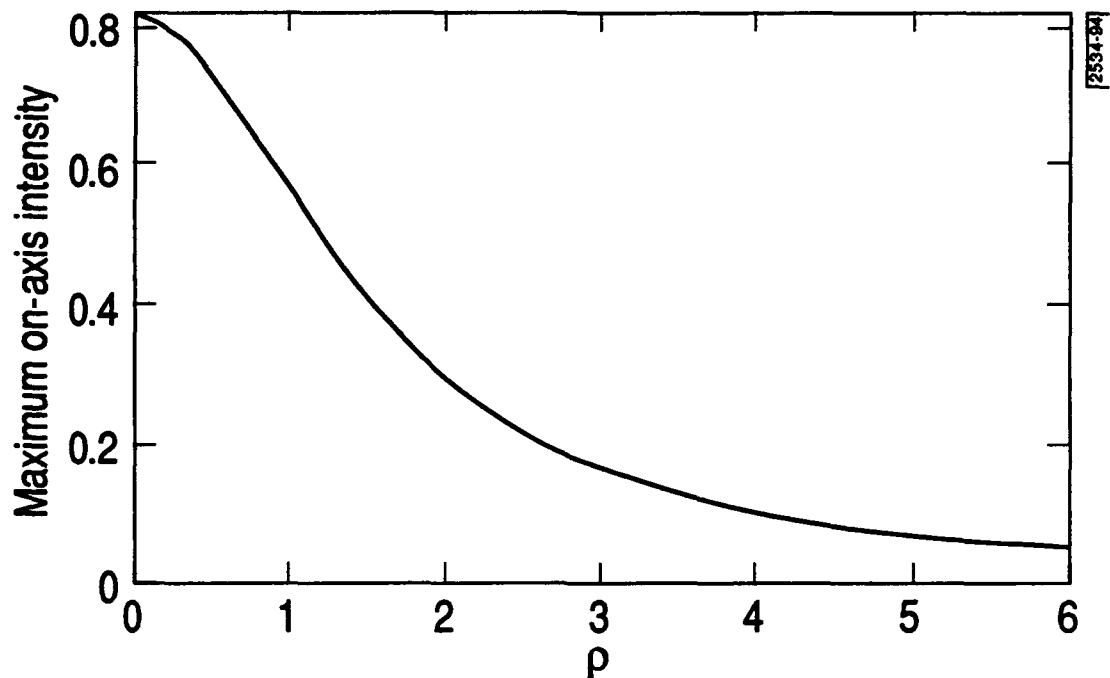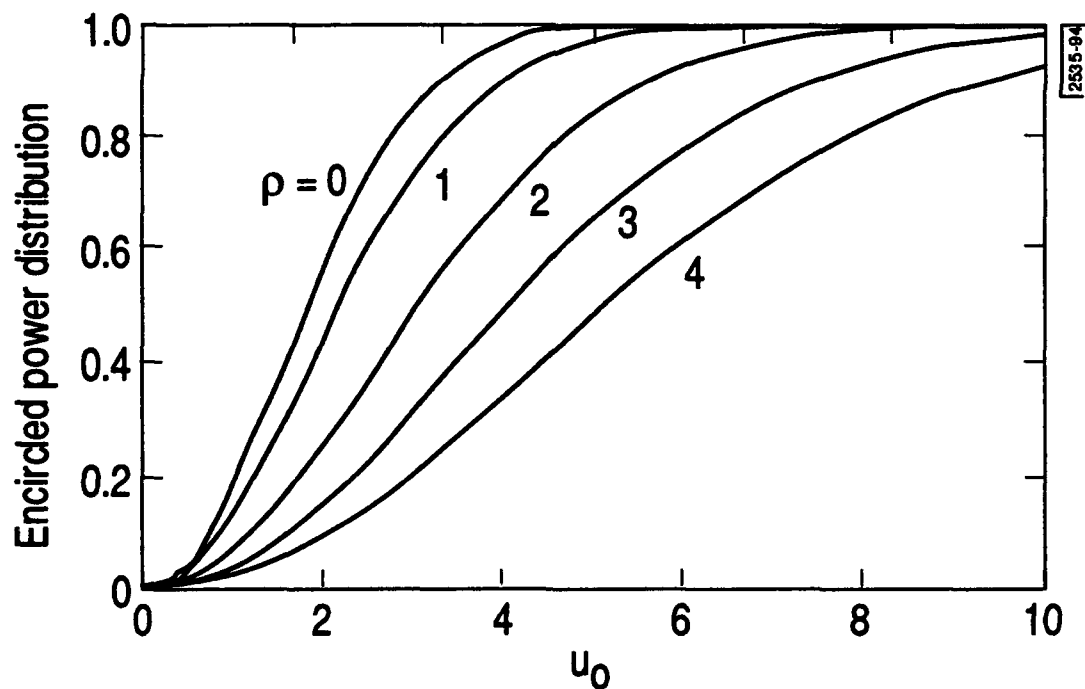In the presence of random angular jitter, we have derived accurate analytical expressions for both the mean far-field irradiance distribution and encircled power for a truncated Gaussian beam that are valid for d/D < 1, where d is the beam diameter in the aperture plane, and D is the truncation diameter. In particular, the mean irradiance distribution gives both the exact on-axis mean irradiance, total integrated transmitted power, and encircled power distribution, valid to better than about 2%. Over the range of interest, the difference between the exact and approximate results are well within the uncertainties that always exist in practice. Based on the approximate irradiance distribution given by Eq. (3.2), we then obtained results for both the optimum ratio of d/D that results in the maximum mean on-axis irradiance and the corresponding on-axis irradiance. As such, the results obtained here will, in many cases, be useful in facilitating parametric estimation and optimization of overall system design.

References

1. V. A. Banakh and V. L. Mironov, "LIDAR in a Turbulent Atmosphere," Chap. 3, Artech House, Inc., Norwood MA (1987).

2. A. E. Siegman, *LASERS*, Sec. 18.4, University Science books, Mill Valley CA (1989).

3. V. N. Mahajan, "Uniform versus Gaussian beams: a comparison of the effects of diffraction, obscuration, and aberrations," *J. Opt. Soc. Am.* A 3, 470–485 (1986).

4. D. L. Fried, "Statistics of laser beam fade induced by pointing jitter," *Appl. Opt.* 12, 422–423 (1973).

5. M. H. Leed and J. F. Holmes, "Effect of the turbulent atmosphere of the autocovariance function for a speckle field generated by a laser beam with random pointing error," *J. Opt. Soc. Am.* 71, 559–565 (1981).

6. H. T. Yura, "Ladar detection statistics in the presence of pointing errors," TR-93(3505)-1, 15 December 1993, The Aerospace Corporation, to be published in *Applied Optics* (Oct. 1994).

TECHNOLOGY OPERATIONS

The Aerospace Corporation functions as an "architect-engineer" for national security programs, specializing in advanced military space systems. The Corporation's Technology Operations supports the effective and timely development and operation of national security systems through scientific research and the application of advanced technology. Vital to the success of the Corporation is the technical staff's wide-ranging expertise and its ability to stay abreast of new technological developments and program support issues associated with rapidly evolving space systems. Contributing capabilities are provided by these individual Technology Centers:

Electronics Technology Center: Microelectronics, solid-state device physics, VLSI reliability, compound semiconductors, radiation hardening, data storage technologies, infrared detector devices and testing; electro-optics, quantum electronics, solid-state lasers, optical propagation and communications; cw and pulsed chemical laser development, optical resonators, beam control, atmospheric propagation, and laser effects and countermeasures; atomic frequency standards, applied laser spectroscopy, laser chemistry, laser optoelectronics, phase conjugation and coherent imaging, solar cell physics, battery electrochemistry, battery testing and evaluation.

Mechanics and Materials Technology Center: Evaluation and characterization of new materials: metals, alloys, ceramics, polymers and their composites, and new forms of carbon; development and analysis of thin films and deposition techniques; nondestructive evaluation, component failure analysis and reliability; fracture mechanics and stress corrosion; development and evaluation of hardened components; analysis and evaluation of materials at cryogenic and elevated temperatures; launch vehicle and reentry fluid mechanics, heat transfer and flight dynamics; chemical and electric propulsion; spacecraft structural mechanics, spacecraft survivability and vulnerability assessment; contamination, thermal and structural control; high temperature thermomechanics, gas kinetics and radiation; lubrication and surface phenomena.

Space and Environment Technology Center: Magnetospheric, auroral and cosmic ray physics, wave-particle interactions, magnetospheric plasma waves; atmospheric and ionospheric physics, density and composition of the upper atmosphere, remote sensing using atmospheric radiation; solar physics, infrared astronomy, infrared signature analysis; effects of solar activity, magnetic storms and nuclear explosions on the earth's atmosphere, ionosphere and magnetosphere; effects of electromagnetic and particulate radiations on space systems; space instrumentation; propellant chemistry, chemical dynamics, environmental chemistry, trace detection; atmospheric chemical reactions, atmospheric optics, light scattering, state-specific chemical reactions and radiative signatures of missile plumes, and sensor out-of-field-of-view rejection.